Electronic Supplementary Material (ESI) for ChemComm.

Electronic Supplementary Information

Platinum-group-metal quaternary alloys with lattice defects for enhanced oxygen electrocatalysis

Qi Li, * Chenqi Xu, Liangmei Luo, Cunwang Ge, * and Yanqing Wang *

Department of Materials Science, School of Chemistry and Chemical Engineering,

Nantong University, Nantong 226019 Jiangsu, P. R. China

Corresponding author: Dr. Qi Li, E-mail: zhuiqiuzhizhuo@163.com

Experimental Section

2.1. *Chemicals and Reagents*

Potasslum tetrachloroplatinate(K_2PtCl_4, 98%), Potasslum hexachloropalladate(IV) (K_2PdCl_6, Pd≥26.3%), Hydrogen hexachloroiridate(IV) hexahydrate (H_2IrCl_6•$6H_2O$, ≥99%), Potasslum pentachlororuthenate(III) hydrate ($Cl_5H_2K_2ORu$, 99.7%, Ru≥24.5%), $NaBH_4$ were obtained from Aladdin Chemistry Co., Ltd.. Pyrrole and styrene monomer were distilled under reduced pressure before use. All other reagents were of analytical grade. Deionized water was used for all experiments. All starting materials and solvents, unless otherwise specified, were used without further purification.

2.2. *Synthesis of hollow carbon spheres (HCS)*

Briefly, PS mother solution (2 mL) was dispersed into a beaker containing 100 mL deionized water, and then 0.1 mL pyrrole monomer was added under stirring, accompanied by a polymerization process via adding ammonium persulfate solution (20 mmol L^{-1}, 20 mL) drop by drop. After four hours of polymerization, the mixture was filtered and washed with deionized water and ethanol several times. The obtained products were dried at 60 °C in a vacuum oven over night, and then denotes as PS@PPy. A certain amount of PS@PPy was placed in a quartz boat and carbonized at 800 °C using a heating rate of 5 °C min^{-1} for 4 h under flowing N_2. The collected products were denoted as HCNs after cooling down to room temperature.

2.3. *Synthesis of imidazolium-$[Pt(Cl)_6]^{2-}$ precursors*

For the synthesis of $Ag_2[PtCl_6]$, 3 mL (50 mM) of $H_2[PtCl_6]$ solution and 3 mL (0.11 M) $AgNO_3$ solution was mixed, and a brown precipitate appeared immediately. The purpose of this step is to ensure that the $H_2[PtCl_6]$ reacts completely by adding slightly excess $AgNO_3$. The obtained $Ag_2[PtCl_6]$ was washed with deionized water several times and re-dispersed in water for further use.

Briefly, 0.82 g (10 mmol) of 2-methylimidazole and 1.98 g (12 mmol) of 1-bromohexane were added to the round bottom flask with a certain amount of ether. The mixture stirred at room temperature for 24h. The formed 1-hexyl-2-methyl imidazole bromide (denoted as IL-Br) was washed with ethyl acetate and ether several times, followed by drying under vacuum at 60 °C for 24h. Subsequently, the as-synthesized IL-Br was added slowly to $Ag_2[PtCl_6]$ dispersion with a molar ratio of 1.9:1 under agitation to form Pt-containing IL (Pt-IL) via anion-exchange. The imidazolium-$[PtCl_6]^{2-}$ IL aqueous solution was obtained by centrifuging to remove AgBr. Pd-IL, Ir-IL, and Ru-IL aqueous solution were synthesized with the same synthetic procedure except that $K_2[PtCl_6]$ was replaced respectively by $K_2[PdCl_6]$, $H_2[IrCl_6]$, and $K_2[H_2ORuCl_5]$.

2.4. *Synthesis of PtPdRuIr/HCS*

Typically, HCS (20 mg) was added to distilled water (50 mL), and stirring for 10 minutes to form a homogeneous dispersion. Pt-IL, Pd-IL, Ir-IL, and Ru-IL (synthesis and use on the spot) was added to above dispersion with stirring for another 10 minutes. 30 mL $NaBH_4$ (100 mg) aqueous solution was added to above solution drop by drop, and stirring for 12 h. The collected products were filtered with distilled water

and ethanol for several times, and dried at 70 °C vacuum oven over the night. For comparison, PtPdRu/HCS, PtPdIr/HCS, PtPd/HCS, PtRu/HCS, PtIr/HCS, and Pt/HCS synthetic procedures were the same as PtPdRuIr/HCS through the addition of corresponding Pt-group metals precursors, respectively.

2.5. *Characterization*

The structures were carried out with a powder X-ray diffraction (XRD) analysis (Philips X'Pert PRO) with Cu K_α radiation. The morphologies of the samples were characterized by field-emission scanning electron microscopy (FESEM Hitachi S-4700) and high-resolution transmission electron microscopy (HRTEM FEI Tecnai G2 F20) fitted with an energy dispersive spectrometer (EDS) detector and high angle angular dark field-scanning transmission electron microscopy (HAADF-STEM). Microstructure was characterized using spherical aberration corrected TEM (ACTEM, FEI-Themis Z) at 200 kV. The chemical compositions and surface chemistry of the samples were examined using an X-ray photoelectron spectroscopy (XPS-7000) spectrometer with Al K_α radiation.

2.6. *Electrochemical test*

All electrochemical measurements were conducted using a CHI760E electrochemical workstation (Chenhua, Co., Ltd., Shanghai) with a three-electrode system. Hg/HgO (1 M KOH) electrode was used as the reference electrode in 0.1 M KOH electrolyte, and Pt mesh (0.5 cm^2) as a counter electrode. All the potentials appeared in this work were calibrated to the reversible hydrogen electrode (RHE) scale according to $E_{vs\ RHE} = E_{vs}$

$_{Hg/HgO}$ +0.0591pH +0.098. Working electrodes were prepared as follows: The as-prepared PtPdRuIr/HCS (4 mg) was put into a Schering bottles (2.5 mL) containing 5 wt.% Nafion solution (40 μL), deionized water (0.75 mL), and isopropanol (0.25 mL), followed by sonicated for at least 30 min to form a homogenous catalyst ink. For the fabrication of PtPdRu/HCS, PtPdIr/HCS, PtPd/HCS, PtRu/HCS, PtIr/HCS, and Pt/HCS catalyst inks, an identical amount of samples was dispersed in 1 mL of the above mixture solution to prepare the corresponding catalyst inks with the same procedure of PtPdRuIr/HCS. Commercial Pt/C (Johnson Matthey, 20%) catalyst ink was also prepared by using the same method. Then the catalyst suspension (10 μL) was drop-casted onto a polished glassy carbon (GC) electrode surface, followed by drying at 30°C for 12h. A rotating disk electrode (RDE) with a GC disk (0.19625 cm^2) and a rotating ring-disk electrode (Pt-ring surface area: 0.1866 cm^2) with a GC disk (0.2475 cm^2) were adopted to support catalyst, and denote as working electrode. The loading of catalysts was determined to be 0.2 mg cm^{-2}.

The activity of GC electrode was firstly evaluated using cyclic voltammetry (CV) test in $K_3[Fe(CN)_6]$ (1 mM) electrolyte containing KNO_3 (0.5 M) with a scan rate of 50 mV s^{-1} until the redox potential difference between $[Fe(CN)_6]^{3-}$ and $[Fe(CN)_6]^{4-}$ is less than 70 mV prior to next measurements. For ORR, CV tests were carried out in O_2- and N_2-saturated 0.1 M KOH with a sweep rate of 50 mV s^{-1} before real test. RDE tests were measured at a scan rate of 10 mV s^{-1} with O_2 purging at various rotation speeds. The kinetic curves were recorded with a linear sweep voltammetry (LSV) polarization at a rotating speed of 1600 rpm with a scan rate of 10 mV s^{-1}. The

long-term durability was evaluated by potentiostatic test at 0.8 V (vs. RHE) in O_2-saturated 0.1 M KOH electrolyte. The activity durability was examined by an accelerated durability test with 10,000 CV cycles in the range of 0.5–0.9 V (vs. RHE). The test of tolerance to methanol was performed by chronoamperometric measurements at 0.4 V (vs. RHE) in an O_2-saturated 0.1 M KOH solution, followed by the injection of methanol (5 mL) after 200s.

The kinetic current density was calculated from the following equation:

$$1/J = 1/J_K + 1/J_L = 1/J_K + 1/(B\omega^{1/2}) \quad (1)$$

where J is the measured current density, J_K is the kinetic current density, J_L is the diffusion limited current density, ω is the rotation rate of the disk electrode.

Tafel slopes were calculated from the Tafel equation:

$$\eta = a + b\log j \quad (2)$$

where η refers to the overpotential, j represents the measured current density, b is the Tafel slope.

2.7. Zinc-air batteries test

The practical applications of PtPdRuIr/HCS catalyst was evaluated by using a home-made electrochemical device (OMS-T4, Changsha Spring New Energy Technology, Co., Ltd., China). Discharge–charge cycling tests were carried out in LAND testing system (CT2001A, Wuhan, China). Carbon paper was cut into a square shape with a side length of 2 cm, and used as substrate for the air cathode. A certain amount of the PtPdRuIr/HCS catalyst ink or the commercial Pt/C catalyst ink

containing identical amount of RuO_2 catalyst was sprayed on the hydrophobic carbon paper uniformly with a mass loading of 1.5 ± 0.1 mg cm^{-2}. A fresh Zn foil was selected as the anode electrode. The electrolyte consists of 6 M KOH and 0.2 M $Zn(CH_3COO)_2$ and a Whatman glass microfiber filter used as the membrane in the test.

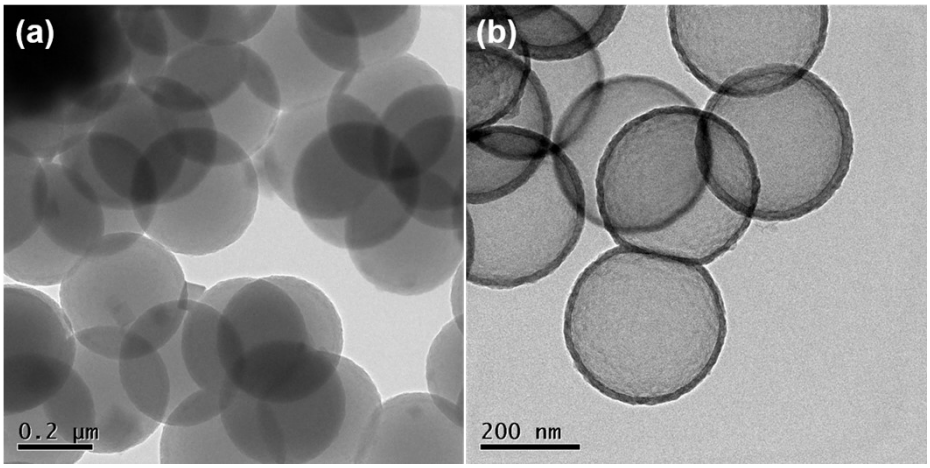

Fig. S1. TEM images of (a) polystyrene@polypyrrole and (b) HCS, respectively.

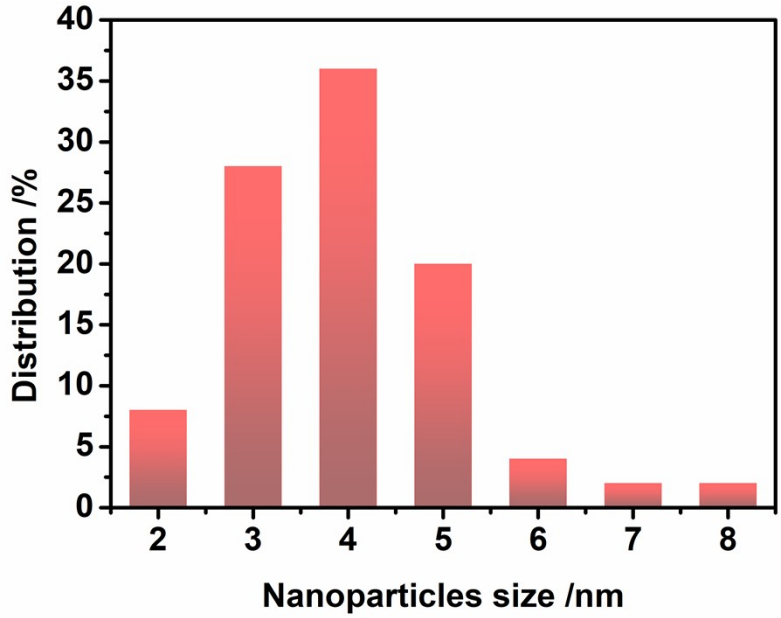

Fig. S2. Size distribution histogram of quaternary alloy PtPdRuIr NPs.

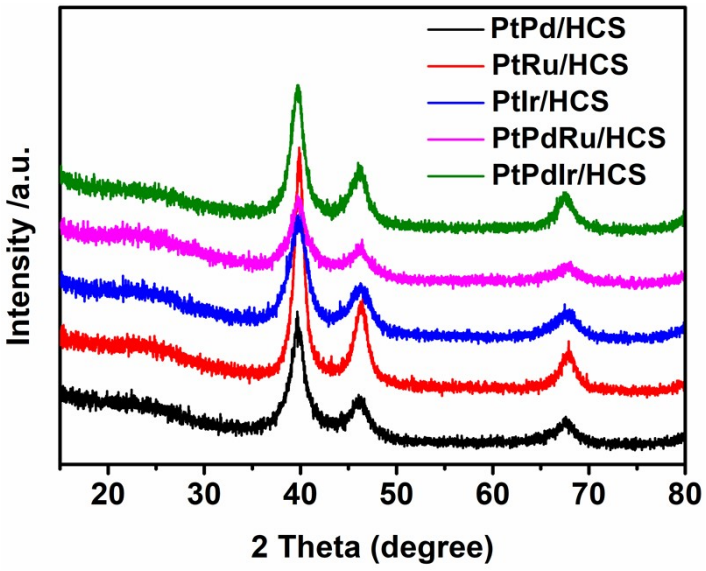

Fig. S3. The XRD patterns of the products.

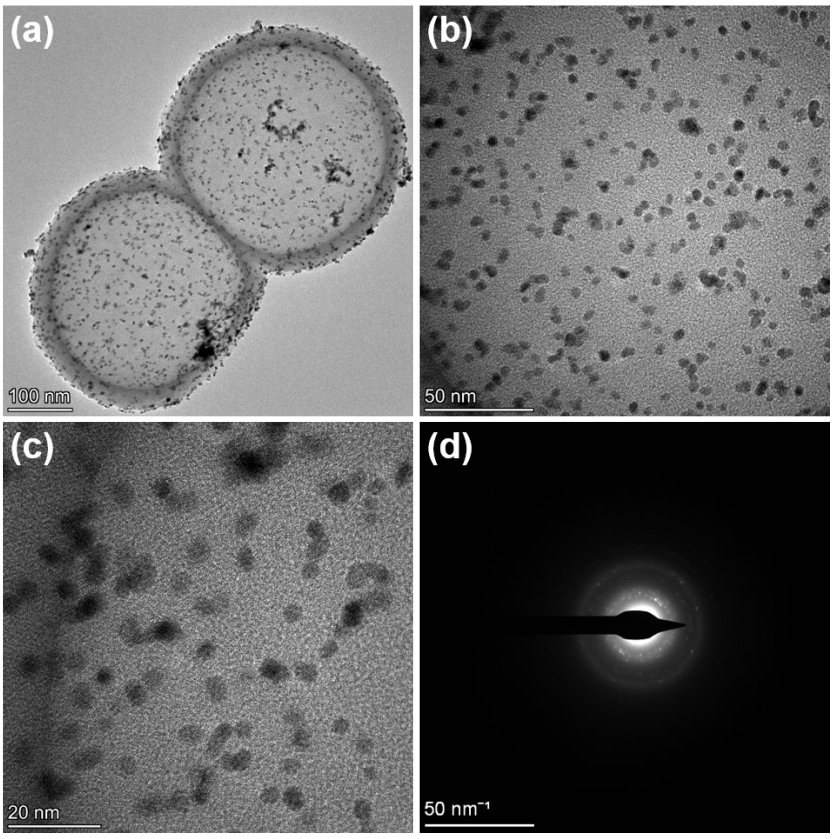

Fig. S4. (a-c) TEM images and (d) SAED image of Pt/HCS.

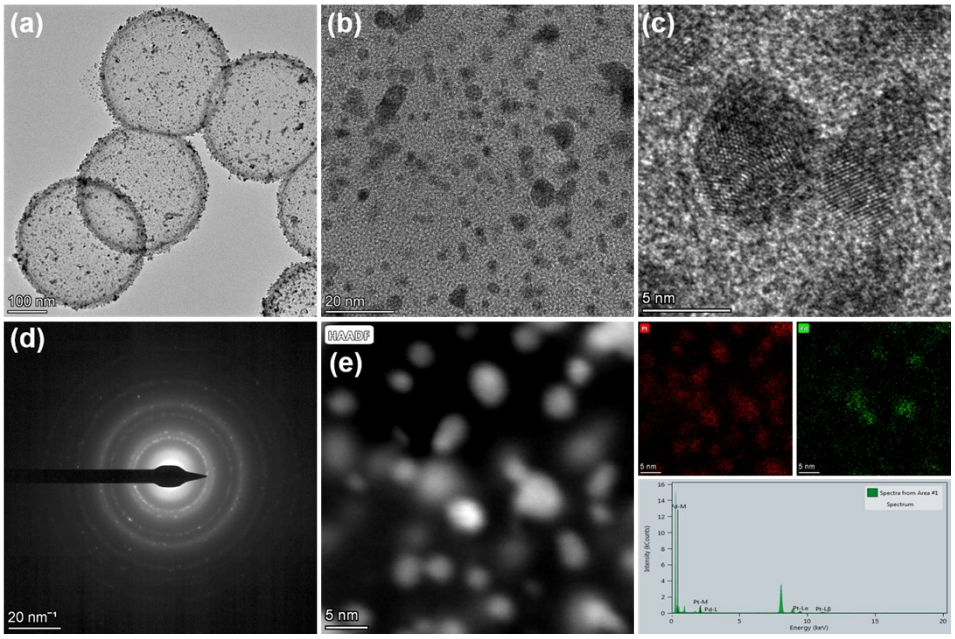

Fig. S5. (a-c) TEM images and (d) SAED image and (e) HAADF-STEM image and corresponding elemental maps and EDX of PtPd/HCS.

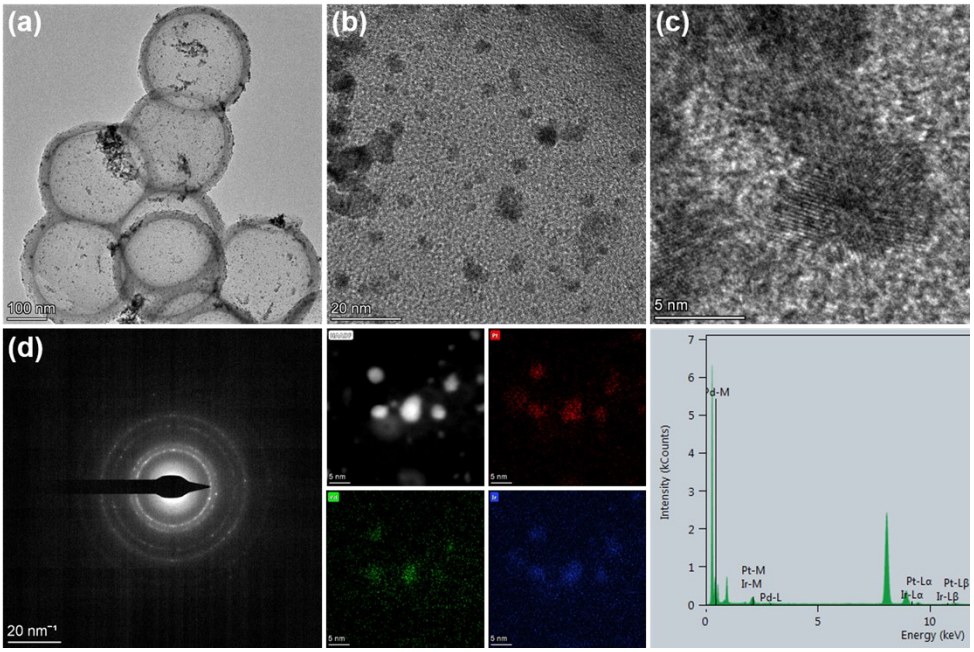

Fig. S6. (a-c) TEM images and (d) SAED image and HAADF-STEM image and corresponding elemental maps and EDX of PtPdiR/HCS.

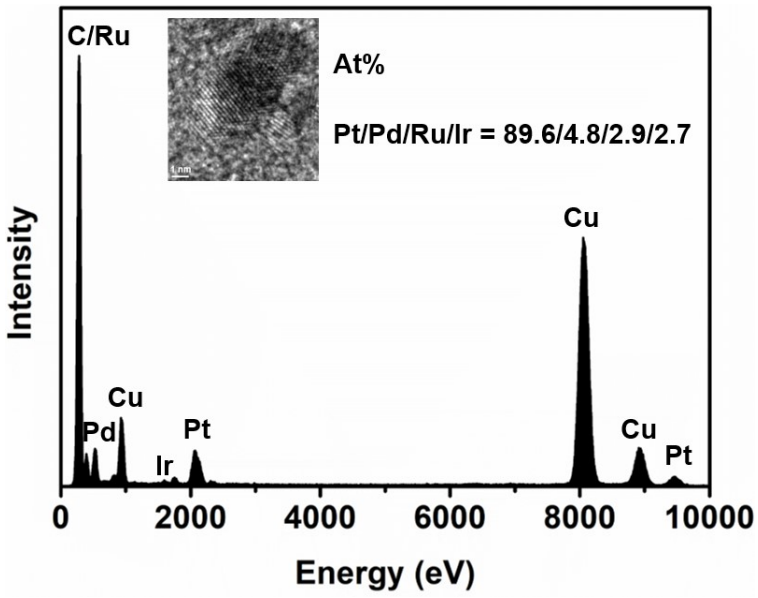

Fig. S7. EDS spectrum of a single PtPdRuIr NPs.

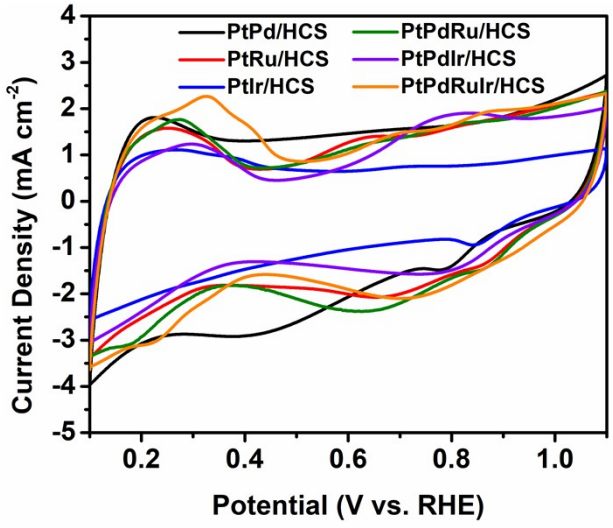

Fig. S8. The CV curves of Pt-group multimetallic catalysts with a scan rate of 20 mV s^{-1} in O_2-saturated 0.1 M KOH solution.

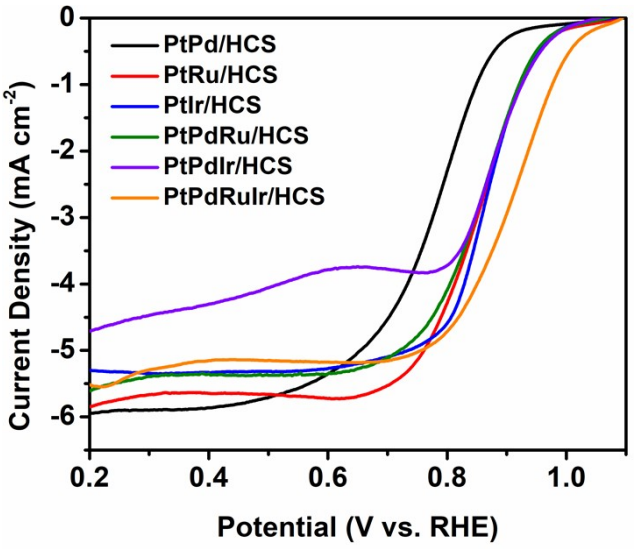

Fig. S9. ORR polarization curves of Pt-group multimetallic catalysts at a rotating speed of 1600 rpm.

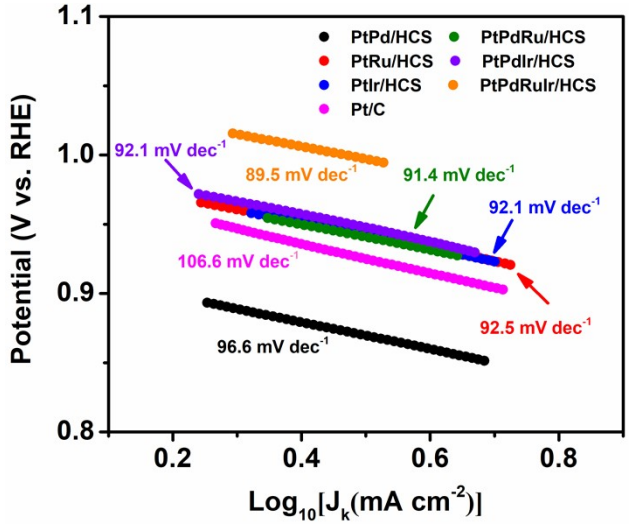

Fig. S10.Tafel slopes of Pt-group multimetallic catalysts.

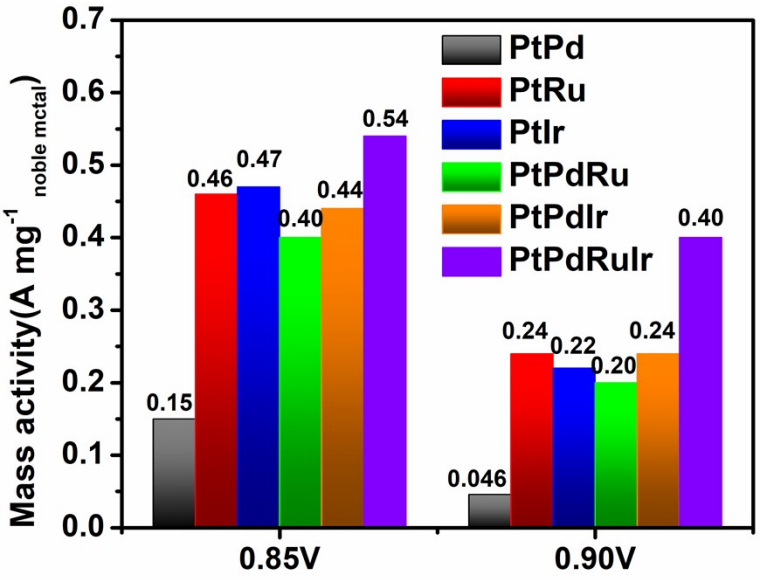

Fig. S11. Mass activity comparisons at 0.85 and 0.9 V, normalized by noble metal loading.

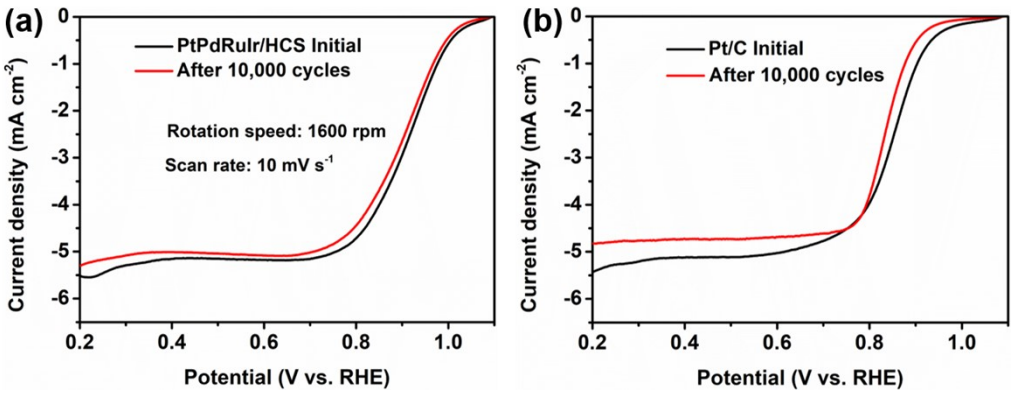

Fig. S12. ORR polarization curves of PtPdRuIr/HCS and com. Pt/C before and after 10,000 CVs

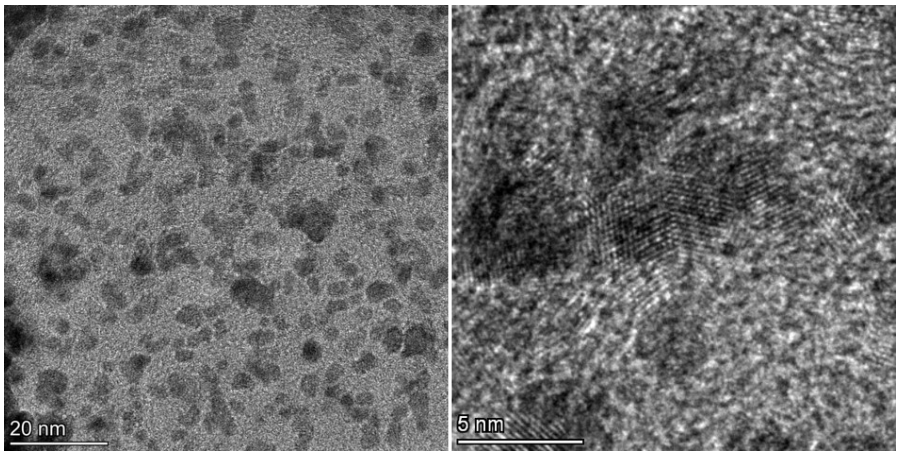

Fig. S13. HAADF-STEM images of PtPdRuIr/HCS after ADT test, proving the morphology of PIFCC-HEI/C maintain well without obvious NP growth and agglomeration.

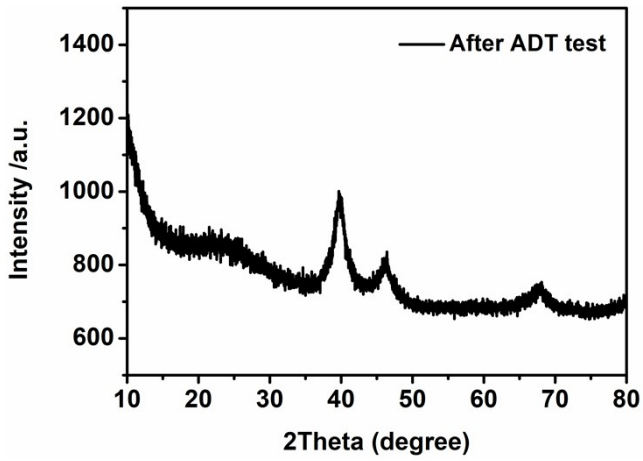

Fig. S14. XRD patterns of PtPdRuIr/HCS nanoparticle after stability test, showing its excellent structural stability

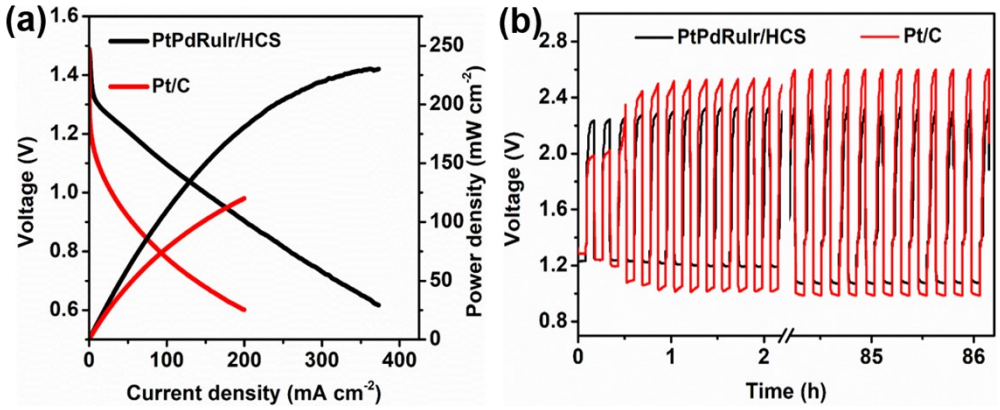

Fig. S15. (a) Discharging polarization plots and the corresponding power density curves of the PtPdRuIr/HCS-based and commercial Pt/C-based zinc-air batteries. (b) Charging–discharging cycle profiles with a current density of 10 mA cm^{-2} and discharging time/charging time of 5/5 min.

To evaluate the practical application potential of the catalysts in energy-storage devices, we assembled a home-made zinc–air battery using PtPdRuIr/HCS and com. Pt/C as catalysts. As displayed in **Fig. S15**, both PtPdRuIr/HCS-based and com. Pt/C-based Zn–air batteries show stable open-circuit voltages near 1.4 V, indicating the reliable activity of the cathode catalyst. Fig. S15a plots the current density–voltage (I–V) polarization and power density profiles of the batteries assembled with PtPdRuIr/HCS and com. Pt/C catalysts. The PtPdRuIr/HCS-based battery delivers higher current densities than the com. Pt/C-based battery over the entire voltage window. The PtPdRuIr/HCS-based battery delivers a current density of 375 mA cm^{-2} at 0.6 V, greatly outperforming the com. Pt/C (200 mA cm^{-2}) Especially, PtPdRuIr/HCS-based battery exhibits the maximum power density (232 mW cm^{-2}), which is considerably higher than that of the com. Pt/C-based battery (125 mW cm^{-2}). Galvanostatic charge–discharge method is used to assess the performance of the Zn–air batteries, and the results are shown in Fig. S15b. The PtPdRuIr/HCS and com. Pt/C-based batteries exhibit high discharge voltage (1.2 V) and similar initial charge voltage. After 500 discharging–charging cycles, the PtPdRuIr/HCS-based battery shows a lower charge–discharge gap than the com. Pt/C-based battery, indicating that

the PtPdRuIr/HCS-based battery has better rechargability than the com. Pt/C-based battery. The PtPdRuIr/HCS-based battery delivers a stable voltage close to the initial discharge voltage. These results confirm that PtPdRuIr/HCS is an excellent catalyst for Zn–air batteries.

Table S1. The element analysis of PtPdRuIr/HCS, which was tested by using the ICP-AES.

Element	At %
Pt	88.2
Pd	3.5
Ru	3.3
Ir	5.0

Table S2. XPS elemental analysis results for the samples.

Samples	Pt^0(Peak/Area)	Pt^{2+}(Peak/Area)	Pt^0(Peak/Area)	Pt^{2+}(Peak/Area)	Pt^0(Percentage %)
Pt/HCS	71.5 eV/103247	72.2 eV/66772	75.0 eV/184864	77.0 eV/41272	72.7
PtPd/HCS	71.5 eV/57030	72.4 eV/40748	75.0 eV/76612	77.0 eV/17306	69.7
PtRu/HCS	71.5 eV/28138	72.2 eV/8416	75.0 eV/16001	77.0 eV/6721	74.5
PtIr/HCS	71.5 eV/64479	72.5 eV/17752	74.9 eV/104907	77.0 eV/26321	79.3
PtPdRu/HCS	71.5 eV/49998	72.4 eV/32437	75.0 eV/72010	77.0 eV/22451	69.0
PtPdIr/HCS	71.4 eV/62862	72.4 eV/30816	74.8 eV/94722	77.0 eV/44213	67.7
PtPdRuIr/HCS	71.6 eV/65056	72.8 eV/12889	75.0 eV/94057	77.0 eV/18404	83.5

Note. The peak area can be directly read from the XPS analysis software.